# Shock-induced ignition for simplified chain-branching kinetics

Josue Melguizo-Gavilanes, Mingjun Tian, Luc Bauwens
Department of Mechanical and Manufacturing Engineering,
University of Calgary, Calgary, T2N1N4, Canada

Zhenhua Pan
State Key Laboratory of Science and Technology on Ballistic,
Nanjing University of Science and Technology,
Nanjing, Jiangsu 210094, China P.R.

## 1 Introduction

The scenario of shock-induced ignition is likely to play a key role in deflagration to detonation transition (DDT). Flame acceleration and reflections over obstacles may result in the presence of a shock wave. Next, after further reflections, that shock will potentially cross over a slow flame, subsequently moving into reactive mixture. Neglecting diffusion, that situation can effectively be reduced to the problem of ignition between a shock and a temperature interface separating reactive from burnt or inert mixture.

Numerical simulation of shock ignition is challenging because the initial conditions are singular, thus initially the region of shocked reactive mixture does not exist. In order to overcome this difficulty and solve the problem accurately and reliably, a combination of techniques has been developed which include replacing space and time as independent variables by the ratio space over time, $\eta = x/t$, and time [1], in addition to using initial conditions obtained from short time asymptotics. The transformation alone, yields a finite domain at $t = 0$ and provides for a well-resolved problem at early times, whereas the short-time asymptotics further improves the treatment of the initial conditions as it allows for a very efficient numerical simulation. The transformed problem is solved using a Weighted-Essentially Non-Oscillatory (WENO) algorithm in space and Runge-Kutta in time, both third order accurate. Results are obtained for a three-step chain-branching kinetic scheme, and show the complete ignition evolution using realistic values of the parameters to properly mimic hydrogen chemistry.

## 2 Physical Model

The problem is governed by the reactive Euler's equations. Chemistry is modeled using a three-step chain-branching scheme originally proposed by Short & Quirk [2]. The three reaction steps are initiation, branching and termination. During the initiation step, the fuel, $\lambda_1$, is converted slowly into chain-radicals, $\lambda_2$. Subsequently, during the branching step, $\lambda_1$ and $\lambda_2$ react to produce more chain-radicals. The reaction

Correspondence to: jmelguiz@ucalgary.ca 

proceeds to completion with the termination step in which the chain-branching specie, $\lambda_2$, is converted into products, $\lambda_3 = 1 - \lambda_1 - \lambda_2$. Initiation and branching are described by an Arrhenius rate, and termination is assumed to be constant. Upon transformation of the governing equations, and using subindex $I$ for initiation, $B$ for branching and $T$ for termination chemistry can be written as:

$$\frac{\partial(t\rho\lambda_1)}{\partial t} + \frac{\partial}{\partial \eta}(\rho u\lambda_1 - \eta\rho\lambda_1) = -t\rho(r_I + r_B) \tag{1}$$

$$\frac{\partial(t\rho\lambda_2)}{\partial t} + \frac{\partial}{\partial \eta}(\rho u\lambda_2 - \eta\rho\lambda_2) = t\rho(r_I + r_B - r_T) \tag{2}$$

where

$$r_I = \lambda_1 \exp\left(\frac{E_I}{T_I} - \frac{E_I}{T}\right),\ r_B = \rho\lambda_1\lambda_2 \exp\left(\frac{E_B}{T_B} - \frac{E_B}{T}\right),\ r_T = k_T\lambda_2 \tag{3}$$

$\rho$ is the density, $u$ is velocity, $p$ is pressure, $e$ is the internal energy, $E$ is the activation energy and $T$ is the temperature. Temperature and internal energy are related to pressure, density, mass fractions, velocity and heat release, $Q$, by

$$p = \rho T, \quad e = \frac{p}{(\gamma - 1)\rho} + \frac{u^2}{2} - Q(1 - \lambda_1 - \lambda_2) \tag{4}$$

Taking the conditions between the contact surface and the shock as a reference, pressure, density and temperature are scaled by their initial postshock values as determined from the inert Riemann problem, velocity by the square root of the ratio pressure/density in the shocked fluid, heat release,internal energy and activation energy by the postshock ratio of pressure/density. Finally, time has been scaled such that the dimensionless constant termination rate is unity. In the transformed problem initial conditions consist of three uniform regions: for $\eta < \eta_s$ (the initial speed of the leading shock), unburnt fluid coming from infinity into the leading shock, shocked mixture for $\eta_s < \eta < 0$ and burnt/inert fluid in the region $\eta > 0$, separated by a temperature jump (i.e. contact surface) located at $\eta = 0$. The dimensionless state ahead of the shock is determined as a function of the shock Mach number using the Rankine-Hugoniot equations. To conclude the physical model, boundary conditions are taken to be consistent with the initial conditions.

## 3 Short-time perturbation solution

Even though the transformation to $\eta$ and $t$ yields a finite domain from $t = 0$, the eigenvalues in this system of coordinates pose an additional challenge as they take the form:

$$\sigma_1 = \frac{u - \eta}{t}, \quad \sigma_2 = \frac{u - \eta + c}{t}, \quad \sigma_3 = \frac{u - \eta - c}{t} \tag{5}$$

where $c$ is the local speed of sound, $c = \sqrt{\gamma p/\rho}$. It is easy to verify that at early times the characteristic speeds approach infinity, which restricts the numerical scheme to very small time steps initially rendering the simulation inefficient. This issue can be amended by either starting the computation at a small positive non-zero time, or more accurately, by using a perturbation model to find an analytical solution at short times which is subsequently used as initial conditions. The perturbation solution is obtained as follows. Typically, initiation is a slow process (i.e. $E_I$ is large), thus for $t = O(1)$, changes in the state variables only occur

at order $\epsilon << 1$ with $\epsilon = \exp(E_I/T_I - E_I)$. Performing the derivation in the original formulation $x$, $t$ (which is easily converted to the $\eta$, $t$ formulation), and using the notation $u'$, $p'$ etc. for perturbations:

$$\frac{\partial \rho'}{\partial t} + \frac{\partial u'}{\partial x} = 0 \tag{6}$$

$$\frac{\partial u'}{\partial t} + \frac{\partial p'}{\partial x} = 0 \tag{7}$$

$$\frac{\partial e'}{\partial t} + \frac{\partial u'}{\partial x} = 0 \tag{8}$$

$$\frac{\partial \lambda_1'}{\partial t} = -1 - a\lambda_2' \tag{9}$$

$$\frac{\partial \lambda_2'}{\partial t} = 1 + a\lambda_2' - \lambda_2' \tag{10}$$

where $e' = T'/(\gamma - 1) + (\lambda_1' + \lambda_2')Q$, and $a = \exp(E_B/T_B - E_B)$. Here, the rate equations can be solved separately, in contrast with single step as derived in Melguizo-Gavilanes et al. [3]. Upon integration of the rate equations, and combining continuity and energy the system reduces to

$$\frac{\partial u'}{\partial t} + \frac{\partial p'}{\partial x} = 0 \tag{11}$$

$$\frac{\partial p'}{\partial t} + \gamma \frac{\partial u'}{\partial x} = -\frac{(\gamma - 1)Q}{a - 1} + \frac{(\gamma - 1)Q}{a - 1} \exp(a - 1)(t + x/V) \tag{12}$$

As boundary conditions we have, at the contact surface, located at $x = 0 + \epsilon x'$, a radiation condition (equivalent to the Riemann variable coming from $x \to +\infty$ being zero) yields $p' - \sqrt{\gamma/T_R}u' = 0$ at $x = 0$. At the shock, located at $x = -Vt + O(\epsilon)$, the Rankine-Hugoniot equations yield a reflection coefficient $Z$ defined by $p' + Zu' = 0$. Rankine-Hugoniot algebra yields:

$$Z = \frac{V[2\gamma + (\gamma - 1)V^2][(\gamma^2 - 2\gamma - 1)V^2 + 2\gamma^2]}{\gamma^2(V^2 + 1)[(\gamma - 3)V^2 + (3\gamma - 1)]} \tag{13}$$

The resulting expressions for $p'$ and $u'$ are:

$$p'(x,t) = \frac{V}{(V^2 - \gamma)(a - 1)} \left\{ \frac{(ZV + \gamma)x + \gamma(Z + V)t - V(t + x/V)(Z + \sqrt{\gamma})\sqrt{\gamma}}{\sqrt{\gamma}(Z + \sqrt{\gamma})} - \frac{1}{(a - 1)} \right.$$
$$\left[ \frac{(Z - \sqrt{\gamma})(V + \sqrt{\gamma})}{2(Z + \sqrt{\gamma})} \exp \frac{(a - 1)(V - \sqrt{\gamma})(x - \sqrt{\gamma}t)}{\sqrt{\gamma}(V + \sqrt{\gamma})} \right.$$
$$\left. \left. + \frac{V - Z}{Z + \sqrt{\gamma}} + \frac{V + \sqrt{\gamma}}{2} \exp \frac{(a - 1)(x + \sqrt{\gamma}t)}{\sqrt{\gamma}} - V \exp(a - 1)(t + x/V) \right] \right\} (\gamma - 1)Q \tag{14}$$

$$u'(x,t) = -\frac{V}{(V^2 - \gamma)(a - 1)} \left\{ \frac{(Z + V)x + (ZV + \gamma)t - (t + x/V)(Z + \sqrt{\gamma})\sqrt{\gamma}}{\sqrt{\gamma}(Z + \sqrt{\gamma})} - \frac{1}{(a - 1)} \right.$$
$$\left[ -\frac{(Z - \sqrt{\gamma})(V + \sqrt{\gamma})}{2\sqrt{\gamma}(Z + \sqrt{\gamma})} \exp \frac{(a - 1)(V - \sqrt{\gamma})(x - \sqrt{\gamma}t)}{\sqrt{\gamma}(V + \sqrt{\gamma})} \right.$$
$$\left. \left. - \frac{V - Z}{Z + \sqrt{\gamma}} + \frac{V + \sqrt{\gamma}}{2\sqrt{\gamma}} \exp \frac{(a - 1)(x + \sqrt{\gamma}t)}{\sqrt{\gamma}} - \exp(a - 1)(t + x/V) \right] \right\} (\gamma - 1)Q \tag{15}$$

Finally, taking the integral of continuity from $t(x) = -x/V$ (i.e. shock) to $t$, an expression for $\rho'(x,t)$ can be found:

$$\rho'(x,t) = \frac{V}{(V^2-\gamma)(a-1)}\left\{\frac{\left[V(Z+V)-(Z+\sqrt{\gamma})\sqrt{\gamma}\right]}{V\sqrt{\gamma}(Z+\sqrt{\gamma})}(t+x/V) - \frac{1}{(a-1)}\right.$$
$$\left[-\frac{Z(V+\sqrt{\gamma})}{\gamma(Z+\sqrt{\gamma})}\exp\frac{(a-1)(V-\sqrt{\gamma})x}{V\sqrt{\gamma}} - \frac{1}{V}\left[\exp(a-1)(t+x/V)-1\right] + \frac{(Z-\sqrt{\gamma})(V+\sqrt{\gamma})}{2\gamma(Z+\sqrt{\gamma})}\right.$$
$$\left.\left.\exp\frac{(a-1)(V-\sqrt{\gamma})(x-\sqrt{\gamma}t)}{\sqrt{\gamma}(V+\sqrt{\gamma})} + \frac{V+\sqrt{\gamma}}{2\gamma}\exp\frac{(a-1)(x+\sqrt{\gamma}t)}{\sqrt{\gamma}}\right]\right\}(\gamma-1)Q \quad (16)$$

## 4 Numerical Simulation

The transformed problem is solved numerically using a third order accurate Weighted Essentially Non-Oscillatory (WENO) algorithm. The code was first developed by Xu et al. [4], and has since been significantly modified and parallelized to handle the shock-ignition problem. It is well-validated, as it has been used successfully in various studies [3, 5–8]. In order to implement the transformation properly a new CFL condition had to be derived as was explained above. The numerical domain goes from a negative value of $\eta$ slightly smaller than $\eta_s$ to a positive value rather larger than the speed of sound behind the contact surface. This guarantees that the leading shock will never reach the left boundary. Likewise, the right boundary is placed at a value greater than the speed of sound behind the contact surface so that acoustic waves moving right will never reach this boundary and no reflection occurs.

## 5 Results

Results shown below were obtained for a shock moving away from the contact surface at a Mach number of 3.8 into a premixed hydrogen-air mixture at ambient conditions, a dimensionless heat release, $Q = 4$, and a ratio of specific heats, $\gamma = 1.4$. Chain-branching parameters for this mixture are $E_B = 8.0$, $E_I = 20$, $T_B = 0.9$, $T_I = 3.0$, and $\epsilon = 1.6196$ x $10^{-6}$. The resolution used for this simulation case was 102,400 grid points for $-2.5 < \eta < 2.5$ which according to [3] is adequate. Figure 1 shows the evolution for pressure and temperature once ignition takes place, the hot spot grows and the reaction wave starts moving towards the leading shock. Since the shock Mach number is relatively high, pressure and temperature disturbances emanating from the reaction zone have time to steepen before reaching the leading shock, and hence a secondary shock forms. The pressure disturbances propagate away from the contact surface at the speed of sound of the postshock state. A careful analysis of Figures 1 and 2 (left) shows that in fact the chain-branched reaction wave lags behind the $p$ disturbances, which lead us to conclude that the reaction wave is propagating subsonically. This outcome in the evolution was also observed by Sharpe & Maflahi [9]. The temperature profiles in Figure 1 (right) show that the contact surface moves backward due to the thermal expansion produced by the chemistry ahead of it. In the current frame of reference, this relative movement indicates that the contact surface is decelerating. Figure 2 (left) shows the evolution of the chain-branching specie, and product, denoted by $\lambda_2$, and $\lambda_3$ respectively. An ignition evolution that is mainly chain-branching in nature is to be expected, as the dimensionless post-shock temperature, $T_s > T_B$, the chain-branching crossover temperature, from the beginning of the simulation. However, since we are pretty close to the limit ($T_B = 1.0$), significant overlapping between chain-branching and termination is observed for profiles from times 10.833 to 11.722. A direct consequence of this, can be seen in the pressure profiles, as the pressure maximum is not located right after the secondary shock forms. Once the shock gains

strength and the reaction zone couples with it, a detonation wave appears. For the current case the detonation will develop fully, once the secondary shock overtakes the leading shock, and will continue to propagate into fresh preshock mixture, as shown in Figure 1. Due to the strengthening of the secondary shock its postshock temperature is higher, which brings an increase in the maximum of $\lambda_2$ as time progresses. The explosion region becomes more chain-branching in nature as the overlap is not as strong at later times. The last profiles for $\lambda_2$, and $\lambda_3$ show this evolution clearly. The pressure maximum is observed to move closer to the shock, hence the reaction zone becomes thinner. The pV-diagram in Figure 2 (right), clarifies the evolution. As explained by Clarke & Nikiforakis [10], it consists of the lead shock wave, an induction region (which has negative slope in the pV-plane), an explosion zone where pressure attains a maximum value, and a termination region where pressure and density decreases (specific volume increases). The exothermic termination region, behaves like a reaction wave, and since it is expansive is a fast flame. Also, the process is unsteady because the negative slopes exhibit a very pronounced curvature [10]. The increase present in the slopes of the secondary shock and the fast-flame region indicates that these zones are accelerating [10].

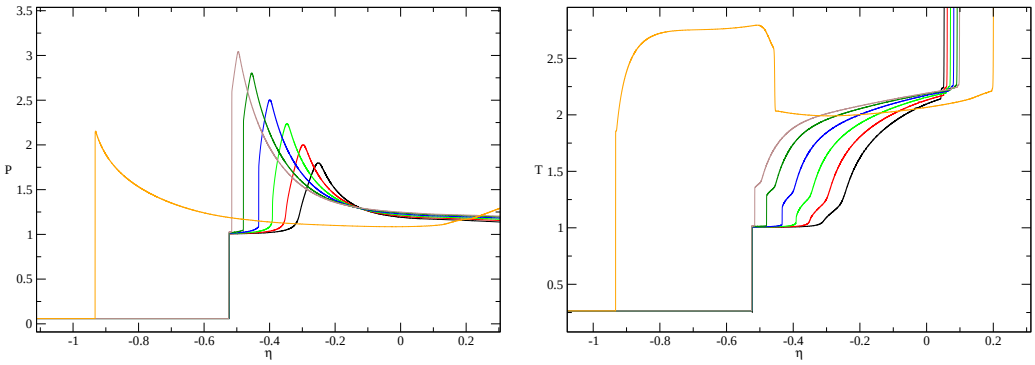


Figure 1: Transition to detonation at times t = 10.833, 11.269, 11.722, 12.194, 12.684, 13.039, and 19.269. Left: Pressure profiles. Right: Temperature profiles.

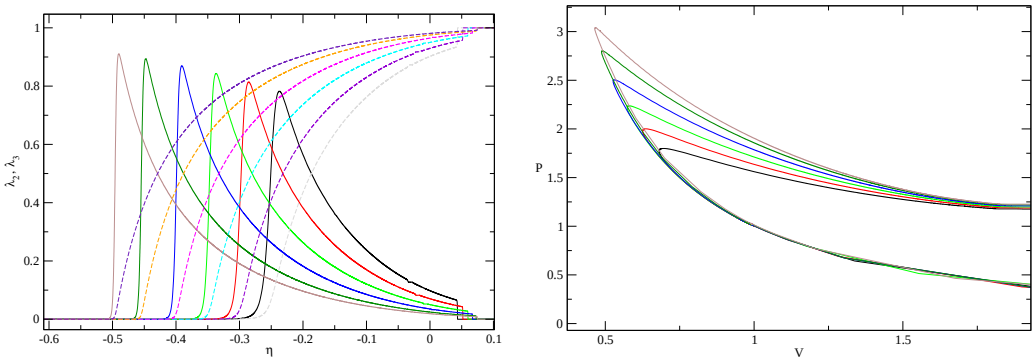


Figure 2: Transition to detonation at times t = 10.833, 11.269, 11.722, 12.194, 12.684 and 13.039. Left: chain-branching specie (solid lines) and product (dashed lines). Right: pV-diagrams

## 6 Conclusion

The scenario of shock-induced ignition was analyzed using a three-step chain-branching kinetic scheme which attempts to model properly the key feature of hydrogen mixtures. In order to handle adequately the singular nature of the initial conditions, the problem was solved in a transformed system of coordinates, namely $\eta$ and $t$, which yields a finite domain from $t = 0$. A detailed derivation of the short-time perturbation used as initial conditions was presented. Its implementation reduced the computational time dramatically, and improved the reliability of the results obtained from the simulations. The ignition process was fully explained based on pressure, temperature, chemical species, and pV diagrams. The propagation of pressure and temperature disturbances, their steepening into a secondary shock, and subsequent transition to detonation was properly captured by our current framework. A detailed parametric analysis of this chemical scheme is currently being carried out.

## References

[1] Short, M., Dold, W. (1996) Unsteady gasdynamic evolution of an induction domain between a contact surface and a shock wave. I: Thermal Runaway, SIAM J. Appl. Math., 56: 1295-1316.

[2] Short, M., Quirk, J.J. (1997) On the non-linear stability and detonability limit of a detonation wave for a model three-step chain-branching reaction, J. Fluid Mech., 339:89-119.

[3] Melguizo-Gavilanes, J., Rezaeyan, N., Lopez-Aoyagi, M. and Bauwens, L. (2010) Simulation of shock-initiated ignition. Shock Waves, doi:10.1007/s00193-010-0255-1.

[4] Xu, S.J., Aslam, T., Stewart, D.S. (1997) High resolution numerical simulation of ideal and non-ideal compressible reacting flows with embedded internal boundaries. Combust. Theor. Model., 1:113-142.

[5] Liang, Z. and Bauwens, L. (2005) Cell structure and stability of detonations with a pressure dependent chain-branching reaction rate model Combust. Theor. Model., 9: 193-112.

[6] Bédard-Tremblay, L., Melguizo-Gavilanes, J. and Bauwens, L. (2009) Detonation structure under chain-branching kinetics with small initiation rate, Proc. Combust. Inst., 32: 2339-2347.

[7] Bédard-Tremblay, L., Fang, L., Melguizo-Gavilanes, J., Bauwens, L., Finstad, P.H.E., Cheng, Z. and Tchouvelev, A.V. (2009) Simulation of detonation after an accidental hydrogen release in enclosed environments, Int. J. Hydrogen Energ., 34: 5894-5901.

[8] Bauwens, L., Bauwens, C.R.L. and Wierzba, I. (2009) Oscillating flames: multiple scale analysis, Proc. R. Soc. Lond. A, 465: 2089-2110.

[9] Sharpe, G.J., Maflahi, N. (2006) Homogeneous explosion and shock initiation for a three-step chain-branching reaction model, J.Fluid Mech., 566:163-194.

[10] Clarke, J.F., Nikiforakis, N.N. (1999) Remarks on diffusionless combustion, Phil. Trans. R. Soc. Lond. A, 357:3605-3620.